

# Measurement of branching fractions for the inclusive Cabibbo-favored $\bar{K}^{*0}(892)$ and Cabibbo-suppressed $K^{*0}(892)$ decays of neutral and charged $D$ mesons

M. Ablikim<sup>1</sup>, J. Z. Bai<sup>1</sup>, Y. Ban<sup>11</sup>, J. G. Bian<sup>1</sup>, X. Cai<sup>1</sup>, J. F. Chang<sup>1</sup>, H. F. Chen<sup>16</sup>, H. S. Chen<sup>1</sup>, H. X. Chen<sup>1</sup>, J. C. Chen<sup>1</sup>, Jin Chen<sup>1</sup>, Jun Chen<sup>7</sup>, M. L. Chen<sup>1</sup>, Y. B. Chen<sup>1</sup>, S. P. Chi<sup>2</sup>, Y. P. Chu<sup>1</sup>, X. Z. Cui<sup>1</sup>, H. L. Dai<sup>1</sup>, Y. S. Dai<sup>18</sup>, Z. Y. Deng<sup>1</sup>, L. Y. Dong<sup>1a</sup>, Q. F. Dong<sup>15</sup>, S. X. Du<sup>1</sup>, Z. Z. Du<sup>1</sup>, J. Fang<sup>1</sup>, S. S. Fang<sup>2</sup>, C. D. Fu<sup>1</sup>, H. Y. Fu<sup>1</sup>, C. S. Gao<sup>1</sup>, Y. N. Gao<sup>15</sup>, M. Y. Gong<sup>1</sup>, W. X. Gong<sup>1</sup>, S. D. Gu<sup>1</sup>, Y. N. Guo<sup>1</sup>, Y. Q. Guo<sup>1</sup>, K. L. He<sup>1</sup>, M. He<sup>12</sup>, X. He<sup>1</sup>, Y. K. Heng<sup>1</sup>, H. M. Hu<sup>1</sup>, T. Hu<sup>1</sup>, X. P. Huang<sup>1</sup>, X. T. Huang<sup>12</sup>, X. B. Ji<sup>1</sup>, C. H. Jiang<sup>1</sup>, X. S. Jiang<sup>1</sup>, D. P. Jin<sup>1</sup>, S. Jin<sup>1</sup>, Y. Jin<sup>1</sup>, Yi Jin<sup>1</sup>, Y. F. Lai<sup>1</sup>, F. Li<sup>1</sup>, G. Li<sup>2</sup>, H. H. Li<sup>1</sup>, J. Li<sup>1</sup>, J. C. Li<sup>1</sup>, Q. J. Li<sup>1</sup>, R. Y. Li<sup>1</sup>, S. M. Li<sup>1</sup>, W. D. Li<sup>1</sup>, W. G. Li<sup>1</sup>, X. L. Li<sup>8</sup>, X. Q. Li<sup>10</sup>, Y. L. Li<sup>4</sup>, Y. F. Liang<sup>14</sup>, H. B. Liao<sup>6</sup>, C. X. Liu<sup>1</sup>, F. Liu<sup>6</sup>, Fang Liu<sup>16</sup>, H. H. Liu<sup>1</sup>, H. M. Liu<sup>1</sup>, J. Liu<sup>11</sup>, J. B. Liu<sup>1</sup>, J. P. Liu<sup>17</sup>, R. G. Liu<sup>1</sup>, Z. A. Liu<sup>1</sup>, Z. X. Liu<sup>1</sup>, F. Lu<sup>1</sup>, G. R. Lu<sup>5</sup>, H. J. Lu<sup>16</sup>, J. G. Lu<sup>1</sup>, C. L. Luo<sup>9</sup>, L. X. Luo<sup>4</sup>, X. L. Luo<sup>1</sup>, F. C. Ma<sup>8</sup>, H. L. Ma<sup>1</sup>, J. M. Ma<sup>1</sup>, L. L. Ma<sup>1</sup>, Q. M. Ma<sup>1</sup>, X. B. Ma<sup>5</sup>, X. Y. Ma<sup>1</sup>, Z. P. Mao<sup>1</sup>, X. H. Mo<sup>1</sup>, J. Nie<sup>1</sup>, Z. D. Nie<sup>1</sup>, H. P. Peng<sup>16</sup>, N. D. Qi<sup>1</sup>, C. D. Qian<sup>13</sup>, H. Qin<sup>9</sup>, J. F. Qiu<sup>1</sup>, Z. Y. Ren<sup>1</sup>, G. Rong<sup>1</sup>, L. Y. Shan<sup>1</sup>, L. Shang<sup>1</sup>, D. L. Shen<sup>1</sup>, X. Y. Shen<sup>1</sup>, H. Y. Sheng<sup>1</sup>, F. Shi<sup>1</sup>, X. Shi<sup>1c</sup>, H. S. Sun<sup>1</sup>, J. F. Sun<sup>1</sup>, S. S. Sun<sup>1</sup>, Y. Z. Sun<sup>1</sup>, Z. J. Sun<sup>1</sup>, X. Tang<sup>1</sup>, N. Tao<sup>16</sup>, Y. R. Tian<sup>15</sup>, G. L. Tong<sup>1</sup>, D. Y. Wang<sup>1</sup>, J. Z. Wang<sup>1</sup>, K. Wang<sup>16</sup>, L. Wang<sup>1</sup>, L. S. Wang<sup>1</sup>, M. Wang<sup>1</sup>, P. Wang<sup>1</sup>, P. L. Wang<sup>1</sup>, S. Z. Wang<sup>1</sup>, W. F. Wang<sup>1d</sup>, Y. F. Wang<sup>1</sup>, Z. Wang<sup>1</sup>, Z. Y. Wang<sup>1</sup>, Zhe Wang<sup>1</sup>, Zheng Wang<sup>2</sup>, C. L. Wei<sup>1</sup>, D. H. Wei<sup>1</sup>, N. Wu<sup>1</sup>, Y. M. Wu<sup>1</sup>, X. M. Xia<sup>1</sup>, X. X. Xie<sup>1</sup>, B. Xin<sup>8b</sup>, G. F. Xu<sup>1</sup>, H. Xu<sup>1</sup>, S. T. Xue<sup>1</sup>, M. L. Yan<sup>16</sup>, F. Yang<sup>10</sup>, H. X. Yang<sup>1</sup>, J. Yang<sup>16</sup>, Y. X. Yang<sup>3</sup>, M. Ye<sup>1</sup>, M. H. Ye<sup>2</sup>, Y. X. Ye<sup>16</sup>, L. H. Yi<sup>7</sup>, Z. Y. Yi<sup>1</sup>, C. S. Yu<sup>1</sup>, G. W. Yu<sup>1</sup>, C. Z. Yuan<sup>1</sup>, J. M. Yuan<sup>1</sup>, Y. Yuan<sup>1</sup>, S. L. Zang<sup>1</sup>, Y. Zeng<sup>7</sup>, Yu Zeng<sup>1</sup>, B. X. Zhang<sup>1</sup>, B. Y. Zhang<sup>1</sup>, C. C. Zhang<sup>1</sup>, D. H. Zhang<sup>1</sup>, H. Y. Zhang<sup>1</sup>, J. Zhang<sup>1</sup>, J. W. Zhang<sup>1</sup>, J. Y. Zhang<sup>1</sup>, Q. J. Zhang<sup>1</sup>, S. Q. Zhang<sup>1</sup>, X. M. Zhang<sup>1</sup>, X. Y. Zhang<sup>12</sup>, Y. Y. Zhang<sup>1</sup>, Yiyun Zhang<sup>14</sup>, Z. P. Zhang<sup>16</sup>, Z. Q. Zhang<sup>5</sup>, D. X. Zhao<sup>1</sup>, J. B. Zhao<sup>1</sup>, J. W. Zhao<sup>1</sup>, M. G. Zhao<sup>10</sup>, P. P. Zhao<sup>1</sup>, W. R. Zhao<sup>1</sup>, X. J. Zhao<sup>1</sup>, Y. B. Zhao<sup>1</sup>, H. Q. Zheng<sup>11</sup>, J. P. Zheng<sup>1</sup>, L. S. Zheng<sup>1</sup>, Z. P. Zheng<sup>1</sup>, X. C. Zhong<sup>1</sup>, B. Q. Zhou<sup>1</sup>, G. M. Zhou<sup>1</sup>, L. Zhou<sup>1</sup>, N. F. Zhou<sup>1</sup>, K. J. Zhu<sup>1</sup>, Q. M. Zhu<sup>1</sup>, Y. C. Zhu<sup>1</sup>, Y. S. Zhu<sup>1</sup>, Yingchun Zhu<sup>1e</sup>, Z. A. Zhu<sup>1</sup>, B. A. Zhuang<sup>1</sup>, X. A. Zhuang<sup>1</sup>, B. S. Zou<sup>1</sup>

(BES Collaboration)

<sup>1</sup> Institute of High Energy Physics, Beijing 100049, P.R. China

<sup>2</sup> China Center for Advanced Science and Technology (CCAST), Beijing 100080, P. R. China

<sup>3</sup> Guangxi Normal University, Guilin 541004, P.R. China

<sup>4</sup> Guangxi University, Nanning 530004, P.R. China

<sup>5</sup> Henan Normal University, Xinxiang 453002, P.R. China

<sup>6</sup> Huazhong Normal University, Wuhan 430079, P.R. China

<sup>7</sup> Hunan University, Changsha 410082, P.R. China

<sup>8</sup> Liaoning University, Shenyang 110036, P.R. China

<sup>9</sup> Nanjing Normal University, Nanjing 210097, P.R. China

<sup>10</sup> Nankai University, Tianjin 300071, P.R. China

<sup>11</sup> Peking University, Beijing 100871, P.R. China

<sup>12</sup> Shandong University, Jinan 250100, P.R. China

<sup>13</sup> Shanghai Jiaotong University, Shanghai 200030, P.R. China

<sup>14</sup> Sichuan University, Chengdu 610064, P.R. China

<sup>15</sup> Tsinghua University, Beijing 100084, P.R. China

<sup>16</sup> University of Science and Technology of China, Hefei 230026, P.R. China

<sup>17</sup> Wuhan University, Wuhan 430072, P.R. China

<sup>18</sup> Zhejiang University, Hangzhou 310028, P.R. China

<sup>a</sup> Current address: Iowa State University, Ames, IA 50011-3160, USA.

<sup>b</sup> Current address: Purdue University, West Lafayette, IN 47907, USA.

<sup>c</sup> Current address: Cornell University, Ithaca, NY 14853, USA.

<sup>d</sup> Current address: Laboratoire de l'Accélérateur Linéaire, F-91898 Orsay, France.

<sup>e</sup> Current address: DESY, D-22607, Hamburg, Germany.

(Dated: November 3, 2018)

The branching fractions for the inclusive Cabibbo-favored  $\bar{K}^{*0}$  and Cabibbo-suppressed  $K^{*0}$  decays of  $D$  mesons are measured based on a data sample of  $33 pb^{-1}$  collected at and around the center-of-mass energy of 3.773 GeV with the BES-II detector at the BEPC collider. The branching fractions for the decays  $D^{+(0)} \rightarrow \bar{K}^{*0}(892)X$  and  $D^0 \rightarrow K^{*0}(892)X$  are determined to be  $BF(D^0 \rightarrow \bar{K}^{*0}X) = (8.7 \pm 4.0 \pm 1.2)\%$ ,  $BF(D^+ \rightarrow \bar{K}^{*0}X) = (23.2 \pm 4.5 \pm 3.0)\%$  and  $BF(D^0 \rightarrow K^{*0}X) = (2.8 \pm 1.2 \pm 0.4)\%$ .

An upper limit on the branching fraction at 90% C.L. for the decay  $D^+ \rightarrow K^{*0}(892)X$  is set to be  $BF(D^+ \rightarrow K^{*0}X) < 6.6\%$ .

PACS numbers: 13.20.Fc,13.25.Ft,13.85.Ni,14.40.Lb

## I. INTRODUCTION

Although  $D$  mesons were found 29 years ago [1, 2], the study of charm meson decay properties is still an interesting field. Measurement of branching fractions for the  $D$  meson decay modes containing  $\bar{K}^{*0}(K^{*0})$  in the final states can provide useful information about the relative strength of the Cabibbo-favored and Cabibbo-suppressed  $D$  decays. The total branching fractions for the exclusive  $D$  decay modes containing  $\bar{K}^{*0}$  are summed to be  $BF(D^0 \rightarrow \bar{K}^{*0}X) = (8.1 \pm 0.8)\%$  and  $BF(D^+ \rightarrow \bar{K}^{*0}X) = (23.1 \pm 2.0)\%$  ( $X = \text{any particles}$ ) with the known branching fractions of neutral and charged  $D$  mesons [3]. The measurement of branching fractions for the inclusive Cabibbo-favored decay  $D \rightarrow \bar{K}^{*0}X$  and Cabibbo-suppressed decay  $D \rightarrow K^{*0}X$  can not only serve as an independent check on the sum of the branching fractions for the exclusive  $D$  decay modes containing  $\bar{K}^{*0}$  meson in the final states, which indicates the need to search for new decay modes, but also provides valuable information in understanding the weak decay mechanism. The knowledge of the inclusive  $D$  meson decay properties will also help one to understand  $B$  decays.

This Letter reports the measurement of branching fractions for the inclusive Cabibbo-favored decay  $D \rightarrow \bar{K}^{*0}X$  and Cabibbo-suppressed decay  $D \rightarrow K^{*0}X$  of neutral and charged  $D$  mesons using a double tag method described in Section III, based on an analysis of about  $33 pb^{-1}$  of data collected with the upgraded Beijing Spectrometer (BES-II) in  $e^+e^-$  annihilation at and around  $\sqrt{s} = 3.773$  GeV.

## II. THE BEIJING SPECTROMETER

BES is a conventional cylindrical magnetic detector [4] operated at the Beijing Electron Positron Collider (BEPC) [5]. BESII is the upgraded version of the BES detector [6]. A 12-layer vertex chamber (VC) surrounding the beam pipe provides trigger information. A forty-layer main drift chamber (MDC) located outside the VC performs trajectory and ionization energy loss ( $dE/dx$ ) measurement with a solid angle coverage of 85% of  $4\pi$  for charged tracks. Momentum resolution of  $\sigma_p/p = 1.7\%\sqrt{1+p^2}$  ( $p$  in GeV/c) and  $dE/dx$  resolution of 8.5% for Bhabha scattering electrons are obtained for the data taken at  $\sqrt{s} = 3.773$  GeV. An array of 48 scintillation counters surrounds the MDC and measures

the time of flight (TOF) of charged tracks with a resolution of about 200 ps for the electrons. Surrounding the TOF is a 12-radiation-length, lead-gas barrel shower counter (BSC) operated in limited streamer mode, which measures the energies of electrons and photons over 80% of the total solid angle, and has an energy resolution of  $\sigma_E/E = 0.22/\sqrt{E}$  ( $E$  in GeV), spatial resolutions of  $\sigma_\phi = 7.9$  mrad and  $\sigma_Z = 2.3$  cm for the electrons. Outside of the BSC is a solenoidal magnet which provides a 0.4 T magnetic field in the central tracking region of the detector. Three double-layer muon counters instrument the magnet flux return, and serve to identify muons with momentum greater than 500 MeV/c. They cover 68% of the total solid angle with longitudinal (transverse) spatial resolution of 5 cm (3 cm). End-cap time-of-flight and shower counters extend coverage to the forward and backward regions. A Monte Carlo package based on GEANT3 has been developed for BESII detector simulation and comparisons with data show that the simulation is generally satisfactory [7].

## III. DATA ANALYSIS

### A. Event Selection

For each event it is required that at least 2 (but no more than 10) charged tracks are well reconstructed in the MDC with good helix fits. All tracks, save those from  $K_S^0$  decays, must originate from the interaction region, which requires that for a charged track, the distance of closest approach be less than 2 cm in the  $xy$  plane, and less than 20 cm in the  $z$  direction. For the  $\pi^+$  and  $\pi^-$  from the  $K_S^0$  decay, the secondary vertex position is required to be less than 8 cm in the  $xy$  plane and within  $\pm 20$  cm in the  $z$  direction to the primary interaction point. In addition, in order to optimize the momentum resolution and charged particle identification, a geometry cut  $|\cos\theta| \leq 0.85$  ( $\theta$  is the polar angle of the track) is applied. For the charged particle mass assignment, a combined confidence level calculated using the  $dE/dx$  and TOF measurements is required to be greater than 0.1% for the pion hypothesis. For the kaon identification, the confidence level for the kaon hypothesis is required to be greater than that for the pion hypothesis.

The  $\pi^0$  is reconstructed through the decay  $\pi^0 \rightarrow \gamma\gamma$ . For the  $\gamma$  from  $\pi^0$  decay, the energy deposited in the BSC is required to be greater than 70 MeV; the electromagnetic shower is required to start in the first 5 readout layers; and the angle between the  $\gamma$  and the nearest charged track is required to be greater than  $22^\circ$ .

---

\*Electronic address: chenjc@mail.ihep.ac.cn

## B. Singly Tagged $\bar{D}^0$ and $D^-$

Around the center-of-mass energy of 3.773 GeV, the  $\psi(3770)$  resonance is produced in electron-positron annihilation ( $e^+e^-$ ). The  $\psi(3770)$  lies just above open charm pair production threshold and decays predominantly into  $D\bar{D}$  pairs. If one  $D$  meson is fully reconstructed (this is called a singly tagged  $\bar{D}$  event), the other  $D$  meson must exist on the recoil side. Throughout the paper, charge conjugation is implied.

For the analysis, singly tagged  $\bar{D}$  events are reconstructed in three hadronic  $\bar{D}^0$  decay modes ( $K^+\pi^-$ ,  $K^+\pi^-\pi^-\pi^+$ , and  $K^+\pi^-\pi^0$ ) and in nine  $D^-$  decay modes ( $K^+\pi^-\pi^-$ ,  $K^0\pi^-$ ,  $K^0K^-$ ,  $K^+K^-\pi^-$ ,  $K^0\pi^-\pi^-\pi^+$ ,  $K^0\pi^-\pi^0$ ,  $K^+\pi^-\pi^-\pi^0$ ,  $K^+\pi^+\pi^-\pi^-\pi^-$  and  $\pi^+\pi^-\pi^-$ ). The reconstruction for the singly tagged  $\bar{D}$  events is the same as that used in the previous works [8, 9].

In order to reduce the background and improve the momentum resolution, a center-of-mass energy constraint kinematic fit (1C-fit) is imposed on each  $mKn\pi$  ( $m=0,1,2$ ;  $n=1,2,3,4$ ) combination. For the singly tagged  $\bar{D}$  decay modes with a neutral kaon or a neutral pion in the daughter particles, an additional constraint kinematic fit for the  $K_S^0 \rightarrow \pi^+\pi^-$  or  $\pi^0 \rightarrow \gamma\gamma$  is also performed. The kinematic fit probability  $P(\chi^2)$  is required to be greater than 0.1%. If more than one combination satisfies the criteria in an event, only the combination with the largest  $P(\chi^2)$  is retained.

Fig. 1 and fig. 2 show the invariant mass spectra for  $mKn\pi$  combinations in the singly tagged  $\bar{D}^0$  and  $D^-$  decay modes, which are calculated based on the track momentum vectors from the kinematic fit. A maximum likelihood fit to the mass spectrum with a Gaussian function for the  $\bar{D}$  signal and a special background function (ARGUS background shape multiplied by a polynomial function) [8] to describe backgrounds yields a total number of  $7033 \pm 193 \pm 316$  singly tagged  $\bar{D}^0$  events and  $5321 \pm 149 \pm 160$  singly tagged  $D^-$  events (as well as the numbers for the individual decay channels). The errors on the numbers of events are statistical (first) and systematic (second) where the later is obtained by varying the parameterization of the background.

## C. Doubly Tagged Events

### 1. Inclusive decay $D \rightarrow \bar{K}^{*0}(K^{*0})X$

The inclusive decay  $D \rightarrow \bar{K}^{*0}X$  is reconstructed on the recoil side of the singly tagged  $\bar{D}$ , where the  $\bar{K}^{*0}$  is reconstructed through its decay to  $K^-\pi^+$ . The regions within a  $\pm 3\sigma_{M_D}$  window around the fitted  $\bar{D}$  masses in the invariant mass spectra for  $mKn\pi$  combinations, as shown in fig. 1 and fig. 2, are defined as the singly tagged  $\bar{D}$  signal regions ( $\bar{D}$  tag region), where  $\sigma_{M_D}$  are the standard deviations of the mass spectra. Those outside a  $\pm 4\sigma_{M_D}$  window around the fitted  $\bar{D}$  masses are taken as the sideband background control regions ( $\bar{D}$  sideband).

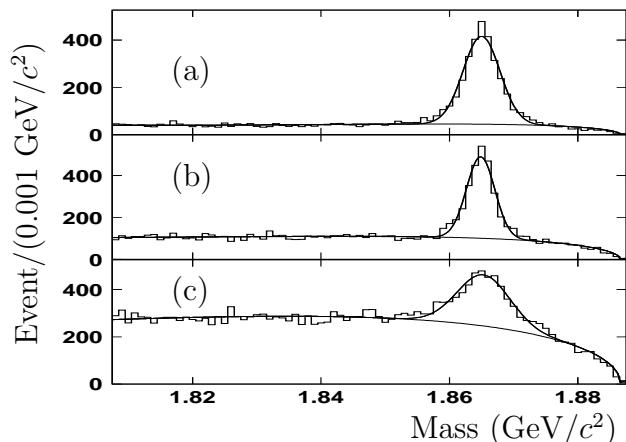


FIG. 1: Invariant mass spectra for  $Kn\pi$  ( $n=1,2,3$ ) combinations in the singly tagged  $\bar{D}^0$  decay modes: (a)  $K^+\pi^-$ , (b)  $K^+\pi^-\pi^-\pi^+$  and (c)  $K^+\pi^-\pi^0$ .

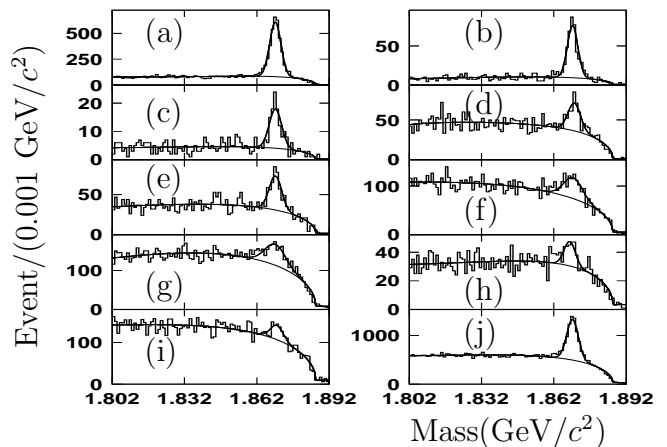


FIG. 2: Invariant mass spectra for  $mKn\pi$  ( $m=0,1,2,n=1,2,3,4$ ) combinations in the singly tagged  $D^-$  decay modes: (a)  $K^+\pi^-\pi^-$ , (b)  $K^0\pi^-$ , (c)  $K^0K^-$ , (d)  $K^+K^-\pi^-$ , (e)  $K^0\pi^-\pi^-\pi^+$ , (f)  $K^0\pi^-\pi^0$ , (g)  $K^+\pi^-\pi^-\pi^0$ , (h)  $K^+\pi^+\pi^-\pi^-\pi^-$ , (i)  $\pi^+\pi^-\pi^-$  and (j) sum of nine modes.

estimation of the number of background events in the  $\bar{D}$  tag region, the number of the events in the  $\bar{D}$  sideband is normalized to the area of the fitted background in the  $\bar{D}$  tag region.

Due to particle misidentification and random combination, the invariant mass for  $K^-\pi^+$  combination could enter into mass spectra more than once per event. To avoid this problem, only the  $K^-\pi^+$  combination with the maximum product of the confidence levels for the  $K$  hypothesis and  $\pi$  hypothesis is retained in an event.

Invariant mass spectra for  $K^-\pi^+$  combinations observed on the recoil side of the  $\bar{D}^0$  tags (the  $mKn\pi$  combinations) are shown in fig. 3 for study of the Cabibbo-favored decay  $D^0 \rightarrow \bar{K}^{*0}X$ , where (a) shows the mass

spectrum for the events with a tagged  $\bar{D}^0$ , and (b) shows the normalized mass spectrum of the  $\bar{D}^0$  sideband events. By fitting the invariant mass spectra for  $K^-\pi^+$  combinations with a Gaussian function for the  $\bar{K}^{*0}$  signal and a polynomial to describe background, the numbers of the observed  $\bar{K}^{*0}$  events are obtained to be  $188.5 \pm 37.3$  and  $92.6 \pm 23.5$  for the tagged and sideband events, respectively. In the fit, the mass and width of  $\bar{K}^{*0}$  are fixed at  $0.8961 \text{ GeV}/c^2$  and  $0.0507 \text{ GeV}/c^2$  quoted from PDG [3], and the detector resolution is set to be  $0.0078 \text{ GeV}/c^2$ , which is obtained by fitting the invariant mass spectrum for  $K^-\pi^+$  combinations from both  $D^0$  and  $D^+$  decays. After subtracting the number of the background events, we obtain  $95.9 \pm 44.1$  signal events for the  $D^0 \rightarrow \bar{K}^{*0}X$  decay.

Similarly, fig. 4 shows the invariant mass spectra for  $K^-\pi^+$  combinations selected on the recoil side of  $D^-$  tags to study the Cabibbo-favored decay  $D^+ \rightarrow \bar{K}^{*0}X$ . Fig. 5 and fig. 6 show the invariant mass spectra for  $K^+\pi^-$  combinations on the recoil side of  $\bar{D}^0$  and  $D^-$  tags to study the Cabibbo-suppressed decays  $D^0 \rightarrow K^{*0}X$  and  $D^+ \rightarrow K^{*0}X$ . With the same analysis procedure as above, the numbers of the observed  $\bar{K}^{*0}/K^{*0}$  events are obtained (Table I). After subtracting the number of the background events, we obtain  $189.1 \pm 36.0$ ,  $30.8 \pm 13.2$  and  $12.3 \pm 23.3$  signal events for  $D^+ \rightarrow \bar{K}^{*0}X$ ,  $D^0 \rightarrow K^{*0}X$  and  $D^+ \rightarrow K^{*0}X$  decays, respectively.

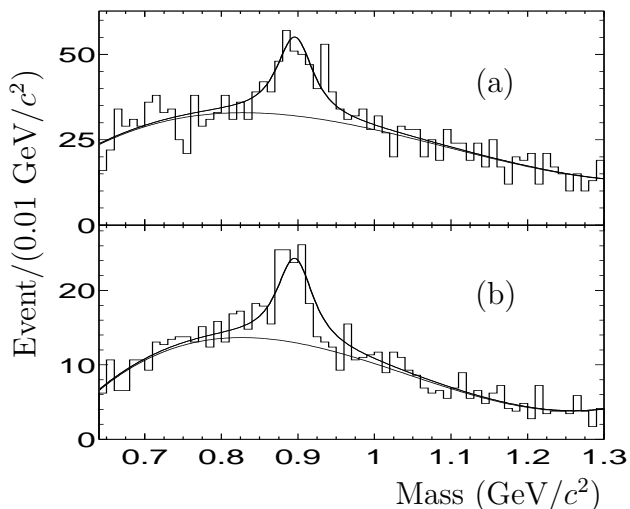


FIG. 3: Invariant mass spectra for  $K^-\pi^+$  combinations observed on the recoil side of the  $\bar{D}^0$  tags for study of the Cabibbo-favored decay  $D^0 \rightarrow \bar{K}^{*0}X$ : (a) the mass spectrum for the events with a  $\bar{D}^0$  tag, (b) the normalized mass spectrum for the  $\bar{D}^0$  sideband events.

## 2. Efficiencies for $D \rightarrow \bar{K}^{*0}(K^{*0})X$

The efficiencies for reconstruction of the inclusive  $\bar{K}^{*0}$  decays of  $D$  mesons are estimated with the Monte Carlo simulation. The Monte Carlo events are generated as

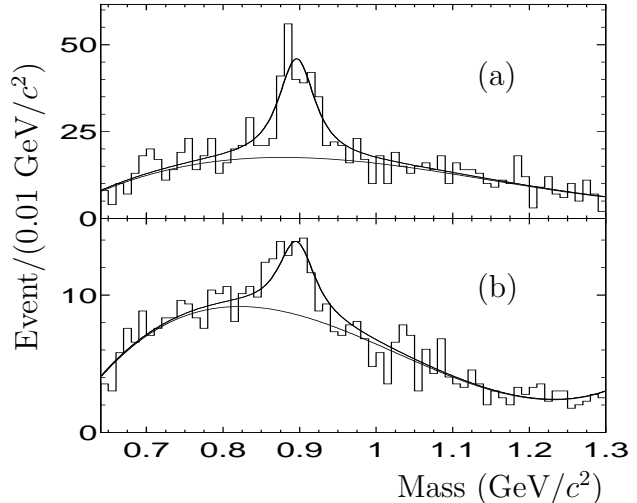


FIG. 4: Invariant mass spectra for  $K^-\pi^+$  combinations observed on the recoil side of the  $D^-$  tags for study of the Cabibbo-favored decay  $D^+ \rightarrow \bar{K}^{*0}X$ : (a) the mass spectrum for the events with a  $D^-$  tag, (b) the normalized mass spectrum for the  $D^-$  sideband events.

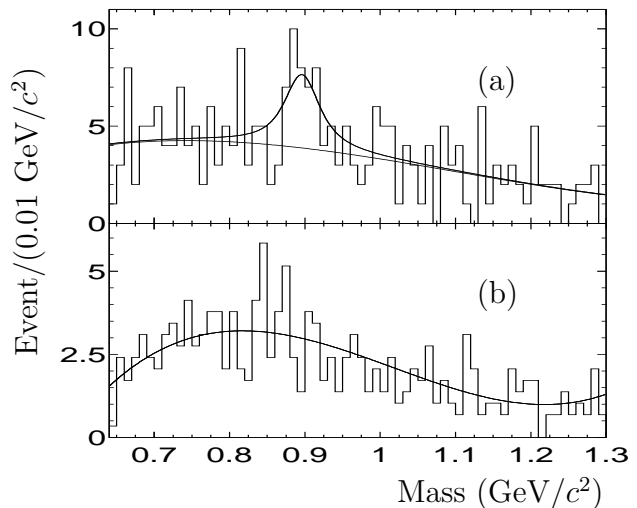


FIG. 5: Invariant mass spectra for  $K^+\pi^-$  combinations observed on the recoil side of the  $\bar{D}^0$  tags for study of the Cabibbo-suppressed decay  $D^0 \rightarrow K^{*0}X$ : (a) the mass spectrum for the events with a  $\bar{D}^0$  tag, (b) the normalized mass spectrum for the  $\bar{D}^0$  sideband events.

$e^+e^- \rightarrow D\bar{D}$ , where  $\bar{D}$  decays into the singly tagged  $\bar{D}$  modes and  $D$  decays into  $\bar{K}^{*0}X$ . The particle trajectories are simulated with the GEANT3 based Monte Carlo simulation package of the BESII detector [7]. The average efficiencies are obtained by weighting the branching fractions of  $D$  meson decays quoted from PDG [3] and the numbers of the singly tagged  $\bar{D}$  events. The efficiencies are  $0.1575 \pm 0.0015$  for the decay  $D^0 \rightarrow \bar{K}^{*0}(K^{*0})X$  and  $0.1529 \pm 0.0021$  for the decay  $D^+ \rightarrow \bar{K}^{*0}(K^{*0})X$ .

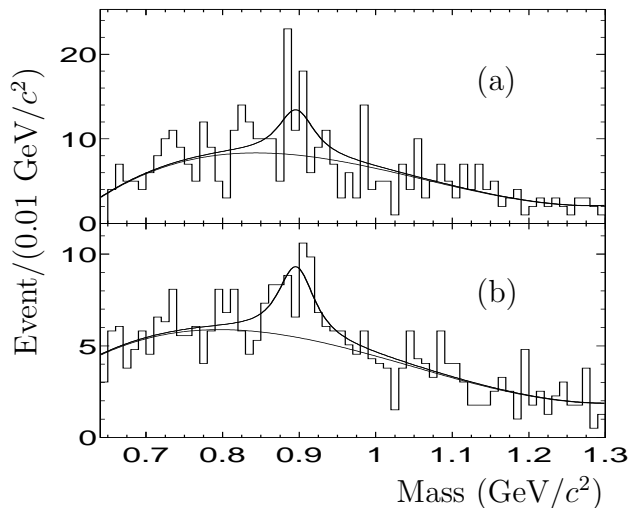


FIG. 6: Invariant mass spectra for  $K^+\pi^-$  combinations observed on the recoil side of the  $D^-$  tags for study of the Cabibbo-suppressed decay  $D^+ \rightarrow K^{*0}X$ : (a) the mass spectrum for the events with a  $D^-$  tag, (b) the normalized mass spectrum for the  $D^-$  sideband events.

TABLE I: Number of  $\bar{K}^{*0}/K^{*0}$  events observed on the recoil side of the  $\bar{D}$  tags, where  $N$  and  $N_b$  are the number of  $\bar{K}^{*0}/K^{*0}$  events observed from the events in which the invariant masses of the  $mK\eta\pi$  combinations are in the  $\bar{D}$  signal region and in the  $\bar{D}$  sideband region, respectively.  $n$  is the number of the signal events for  $D$  decays.

Decay Mode	$N$	$N_b$	$n$
$D^0 \rightarrow \bar{K}^{*0}X$	$188.5 \pm 37.3$	$92.6 \pm 23.5$	$95.9 \pm 44.1$
$D^0 \rightarrow K^{*0}X$	$30.8 \pm 13.2$	$0.0 \pm 0.1$	$30.8 \pm 13.2$
$D^+ \rightarrow \bar{K}^{*0}X$	$232.5 \pm 30.9$	$43.4 \pm 18.4$	$189.1 \pm 36.0$
$D^+ \rightarrow K^{*0}X$	$43.7 \pm 17.6$	$31.4 \pm 15.2$	$12.3 \pm 23.3$

#### IV. RESULTS

With the numbers of the observed signal events for the decay  $D \rightarrow \bar{K}^{*0}X$ , the numbers of the singly tagged  $\bar{D}$  mesons and the reconstruction efficiencies, the branching fractions for the Cabibbo-favored decay  $D \rightarrow \bar{K}^{*0}X$  are determined to be

$$BF(D^0 \rightarrow \bar{K}^{*0}X) = (8.7 \pm 4.0 \pm 1.2)\% \quad (1)$$

and

$$BF(D^+ \rightarrow \bar{K}^{*0}X) = (23.2 \pm 4.5 \pm 3.0)\%. \quad (2)$$

These results are consistent with those measured by the BES collaboration based on the data taken at  $\sqrt{s} = 4.03$  GeV [10].

For the Cabibbo-suppressed decay  $D^0 \rightarrow K^{*0}X$  the branching fraction is obtained to be

$$BF(D^0 \rightarrow K^{*0}X) = (2.8 \pm 1.2 \pm 0.4)\%. \quad (3)$$

An upper limit on the branching fraction at 90% C.L. for the Cabibbo-suppressed decay  $D^+ \rightarrow K^{*0}X$  is set to be

$$BF(D^+ \rightarrow K^{*0}X) < 6.6\%, \quad (4)$$

which includes the systematic uncertainty.

If we treat the observed events as signal events, the branching fraction for the Cabibbo-suppressed decay  $D^+ \rightarrow K^{*0}X$  is

$$BF(D^+ \rightarrow K^{*0}X) = (1.5^{+2.9}_{-1.0} \pm 0.2)\%. \quad (5)$$

In the measured branching fractions, the first error is statistical and second systematic. The systematic error arises from the uncertainties in particle identification ( $\sim 1.0\%$ ) [8], in tracking (2.0% per track), in the numbers of the singly tagged  $\bar{D}^0$  ( $\sim 4.5\%$ ) and  $D^-$  ( $\sim 3.0\%$ ) [8], in background parameterization ( $\sim 12\%$ ), and in Monte Carlo statistics (0.16% for  $D^0$  and 0.31% for  $D^+$ ). These uncertainties are added in quadrature to obtain the total systematic error, which is 13.5% for the  $D^0$  decay and 13.0% for the  $D^+$  decay.

#### V. SUMMARY

Based on an analysis of about  $33 \text{ pb}^{-1}$  of data collected with the BES-II detector at the BEPC collider, we measured branching fractions for the inclusive Cabibbo-favored decay  $D \rightarrow \bar{K}^{*0}X$  and Cabibbo-suppressed decay  $D \rightarrow K^{*0}X$ . The results are  $BF(D^0 \rightarrow \bar{K}^{*0}X) = (8.7 \pm 4.0 \pm 1.2)\%$ ,  $BF(D^+ \rightarrow \bar{K}^{*0}X) = (23.2 \pm 4.5 \pm 3.0)\%$  and  $BF(D^0 \rightarrow K^{*0}X) = (2.8 \pm 1.2 \pm 0.4)\%$ . We set an upper limit on the branching fraction at 90% C.L. for the decay  $D^+ \rightarrow K^{*0}X$  to be  $BF(D^+ \rightarrow K^{*0}X) < 6.6\%$ .

#### VI. ACKNOWLEDGMENTS

The BES collaboration thanks the staff of BEPC for their diligent efforts. This work is supported in part by the National Natural Science Foundation of China under contracts Nos. 10491300, 10225524, 10225525, the Chinese Academy of Sciences under contract No. KJ 95T-03, the 100 Talents Program of CAS under Contract Nos. U-11, U-24, U-25, and the Knowledge Innovation Project of CAS under Contract Nos. U-602, U-34 (IHEP); and by the National Natural Science Foundation of China under Contract No. 10175060 (USTC), and No. 10225522 (Tsinghua University).

[1] G. Goldhaber, et al., Phys. Rev. Lett.**37** (1976) 255.

[2] I. Peruzzi, et al., Phys. Rev. Lett.**37** (1976) 569.

- [3] S. Eidelman et al. (Particle Data Group), Phys. Lett. **B 592** (2004) 1-1109.
- [4] J.Z. Bai et al, Nucl. Instr. and Methods **A344** (1994) 319.
- [5] M. H. Ye and Z.P. Zheng, Proceeding of the XIV International Symposium on Lepton and Photon Interaction, Stanford, California, 1989 (World Scientific, Singapore, 1990).
- [6] J.Z. Bai et al, Nucl. Instr. and Methods **A458** (2001) 627.
- [7] M. Ablikim et al, physics/0503001, to be published in Nuclear Inst. and Methods **A**.
- [8] M. Ablikim et al, Phys. Lett. **B597** (2004) 39-46.
- [9] M. Ablikim et al, Phys. Lett. **B608** (2005) 24-30.
- [10] Gang Rong (for BES collaboration), Proceedings of the 29th International Conference on High Energy Physics (ICHEP'98), Vancouver, Canada, July 23-29,1998.